Materials Physics and Mechanics. 2022;48(3): 428-442
Research article
http://dx.doi.org/10.18149/MPM.4832022_13

Submitted: January 9, 2022
Approved: May 26, 2022
Accepted: June 6, 2022

Seismic behavior of heritage building with isotropic and orthotropic material properties: a comparative analysis

Kamran[1]✉, Shakeel Ahmad[2], Rehan A. Khan[2]

[1]Department of Civil Engineering, Indian Institute of Technology Roorkee, Roorkee 247667, India

[2]Department of Civil Engineering, Aligarh Muslim University, Aligarh 202002, India

✉ kmrn890@gmail.com

Abstract. Restoration and retrofitting of heritage buildings is a complex analysis. In actual practice, building materials of heritage masonry buildings are anisotropic. However, in practice, these building materials had been considered isotropic to optimize the analysis. The present study is a comparative analysis of these two approaches. A heritage school building in northern India underlying seismic zone IV has been considered for the analysis. The seismic performance analysis of the buildings has been carried out through numerical modeling using the SAP2000. Analysis has been carried out for one set of isotropic and three sets of orthotropic material parameters. Normal and shear stresses had been observed and compared with stress calculated from the empirical relationships provided in the standard code of practice.

Keywords: heritage building, orthotropic material, seismic performance, Chamoli earthquake, modal analysis

Acknowledgements*. The authors are highly grateful to UGC for providing grants (File no. 3.44/2012 (SAP II)) for undertaking this work.*

Citation: Kamran, Ahmad S, Khan RA. Seismic behavior of heritage building with isotropic and orthotropic material properties: a comparative analysis. *Materials Physics and Mechanics*. 2022;48(3): 428-442. DOI: 10.18149/MPM.4832022_13.

1. Introduction

The understanding of the failure mechanism of masonry structures under lateral loads is of utmost importance, as it fails miserably under lateral load [1-5]. Doors and windows opening are highly vulnerable [6]. The investigation of seismic behaviour of any heritage buildings (typically masonry structures) is combined with several difficulties such to find its original design plans. Moreover, modifications have occurred to the structure due to changes of use or combined with renovations over time [7,8]. Unfortunately, documentations on modifications of the structure are also not available either. To find the seismic performance of structures it is very useful to find old records of historical earthquakes in the region. Due to the non-availability of codes at the time of construction, the design of masonry buildings was based on personal experience resulting in very thick and uneconomic structures. In order to minimize the effort of the material survey, parameters must be defined with reference to present codes or reference values of similar structures. Masonry is a composite, non-homogeneous and anisotropic material. It may be of stones, bricks, adobe, or tiles bonded together with mortar. Masonry structures are load-bearing and perform a variety of functions like supporting loads, subdividing space, providing thermal insulation and weather protection, etc. Being a heterogeneous material, behaviour of masonry depends on the mechanical properties of its components, the arrangement of the units, the interfaces between them, and the interaction of these units with other structural members and materials used in the building (e.g. timber or steel beams and columns and timber floors) [9-12].

Camathias U. [13] has conducted theoretical and experimental research and found various parameters of masonry construction which affect the strength, stability, and performance of masonry structures are found, need to be considered in the design. It is a vital issue to understand the lateral load resisting system of such structures for their comprehensive structural analysis. The earthquake waves hitting perpendicular to the longer side of the wall are more vulnerable than that hitting parallel to the longer side of the wall. This is mainly due to the height-to-thickness ratio of the masonry wall [13]. The historic masonry walls have confirmed the high vulnerability and low shear capacity when exposed to seismic actions whereas the shear strength of masonry increases with the pre-compression up to a limit and becomes constant at higher pre-compression [15]. Nowadays, finite element analyses have become the most important tool for the analysis of historical structures [10,16]. Sarhosis V. et al. [17] have found that 3D simulation approach is more reliable to investigate the real seismic response than 2D analysis. Parajuli H.R. [18] investigated the effects of various earthquake ground motions on finite element model (FEM) have confirmed that old masonry structures were found very weak in resisting seismic forces. The article is devoted to the important applied problem – the seismic resistance estimation of ground buildings. Due to the high risks of destruction during the earthquake, the old building should be modified to resist enough stability. In the case of the impossibility to carry out laboratory experiments, computer simulation is a reasonable technique. The nonlinear analysis technique is widely used by other scientific groups [19]. The author described the current state of the art in the direction is seismic impact simulations, however, not only finite-element methods show good results. For example, due to the hyperbolicity of the considered dynamic problem, the grid-characteristic method recently showed perfect precision [20].

In the present study, the seismic behaviour of the masonry heritage school (STS High School, Aligarh) building has been analysed. It is a brick masonry structure, established in 1875 A.D. It is a residential school in seismic zone IV with the strength of 2000 students. Figure 1 shows a northwest view of the school building.

Fig. 1. STS High School Front NorthWest view [21]

2. Mathematical Modelling Techniques

The following modelling techniques can be adopted [10,14].

(1) *Detailed micro modelling*: Units and mortar joints are represented by continuum elements whereas the unit-brick interface is represented by discontinuous elements.

(2) *Simplified Micro modelling*: Expanded units are represented by continuum elements whereas the behaviour of the mortar joints and the unit-mortar interface is lumped in discontinuous elements. These interface elements represent the preferential crack locations where tensile and shear cracking occur.

(3) *Macro-modelling*: Units, mortar, and unit-mortar interface are smeared out in the continuum. It is more practice-oriented due to the reduced time and memory requirements as well as user-friendly mesh generation.

These three types of modelling techniques of a masonry sample have been shown in Fig. 2.

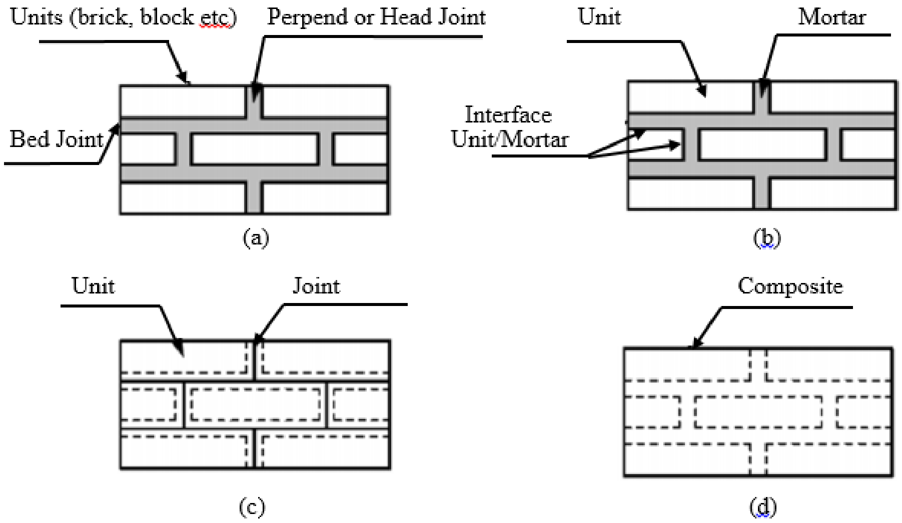

Fig. 2. Modeling Techniques for Brick Masonry (a) typical masonry sample, (b) detailed micro modeling, (c) simplified micro-modeling, (d) macro-modeling [22]

3. Numerical Modeling of the Heritage Building

The case study structure is load-bearing. Since it is a very large structure, the heterogeneous micro modelling is not possible, therefore, the homogeneous macro modelling is used for Finite Element (FE) modelling of the unreinforced masonry heritage structure. Since the ground and first-floor plans are almost similar, see Figs. 3,4 and the building is almost symmetrical, therefore, only half of the building is considered for numerical analysis. It is also a reasonable approach in order to make a computationally efficient finite element model. All the walls in the structure except the veranda walls are 304.8 mm thick while the veranda walls are 228.6 mm thick. The height of the ground floor is 5.13 m and the height of the first floor is 4.65 m while the height of the first floor of veranda wall is 3.84 m. SAP2000 software is used for analysis in which the homogeneous masonry units are modelled using shell elements because it has good agreement with finite element software and experimental results [23]. The building rests on very firm soil with about 1.5 m deep masonry strip footing. The support condition, therefore, is taken as fixed in the software model. Masonry columns are provided in the buildings. Some are solid and some are hollow from the inside. Hollow columns are not considered in the software design model. The building is having an arched roof supported on iron girders which are resting on masonry walls. Columns and iron girders are modeled using frame elements in the software model. The results obtained will be generalized for the whole building. Figure 5 shows 3D view of the software model of the structure with co-ordinate axes.

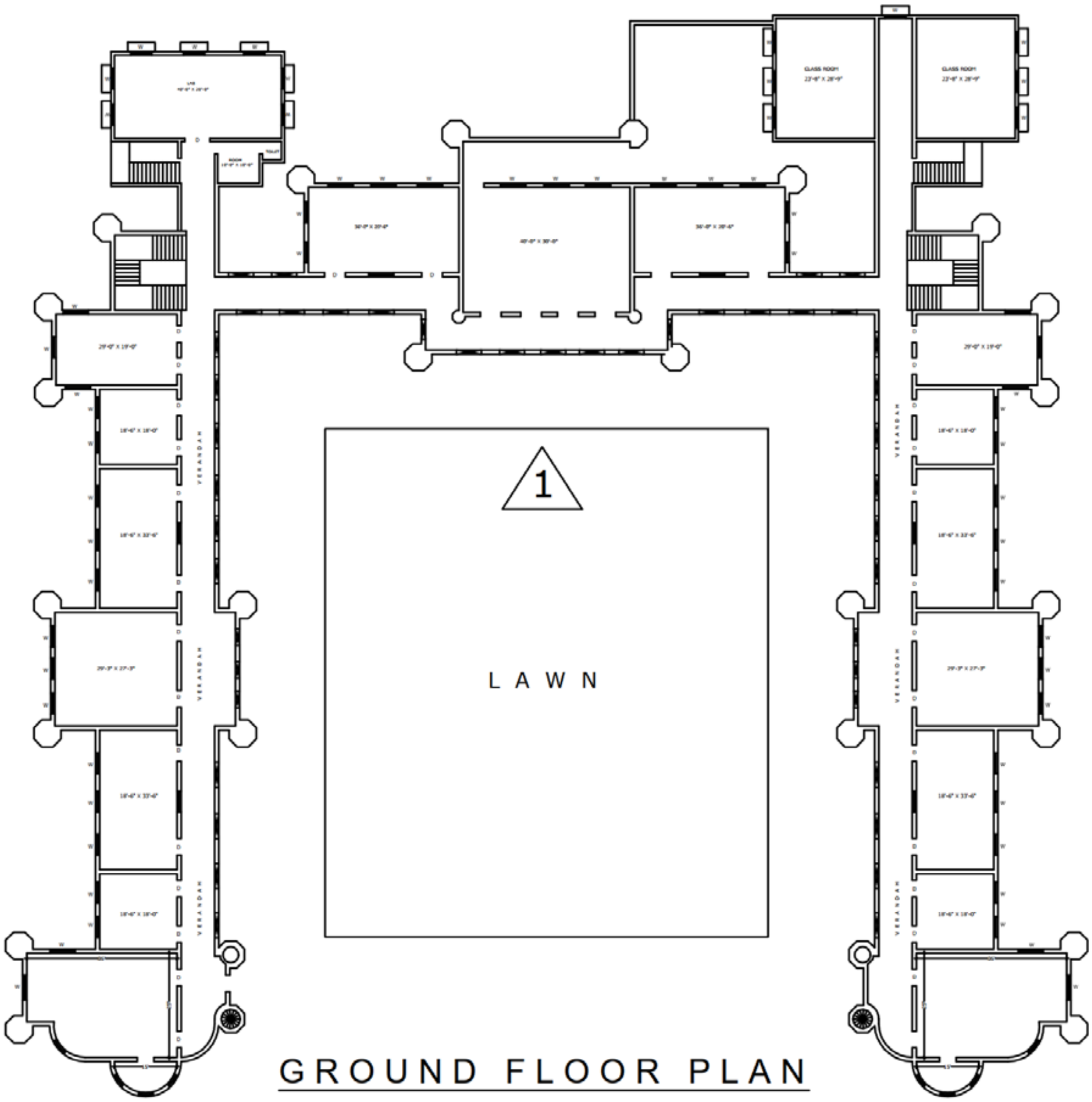

Fig. 3. Typical Ground Floor Plan

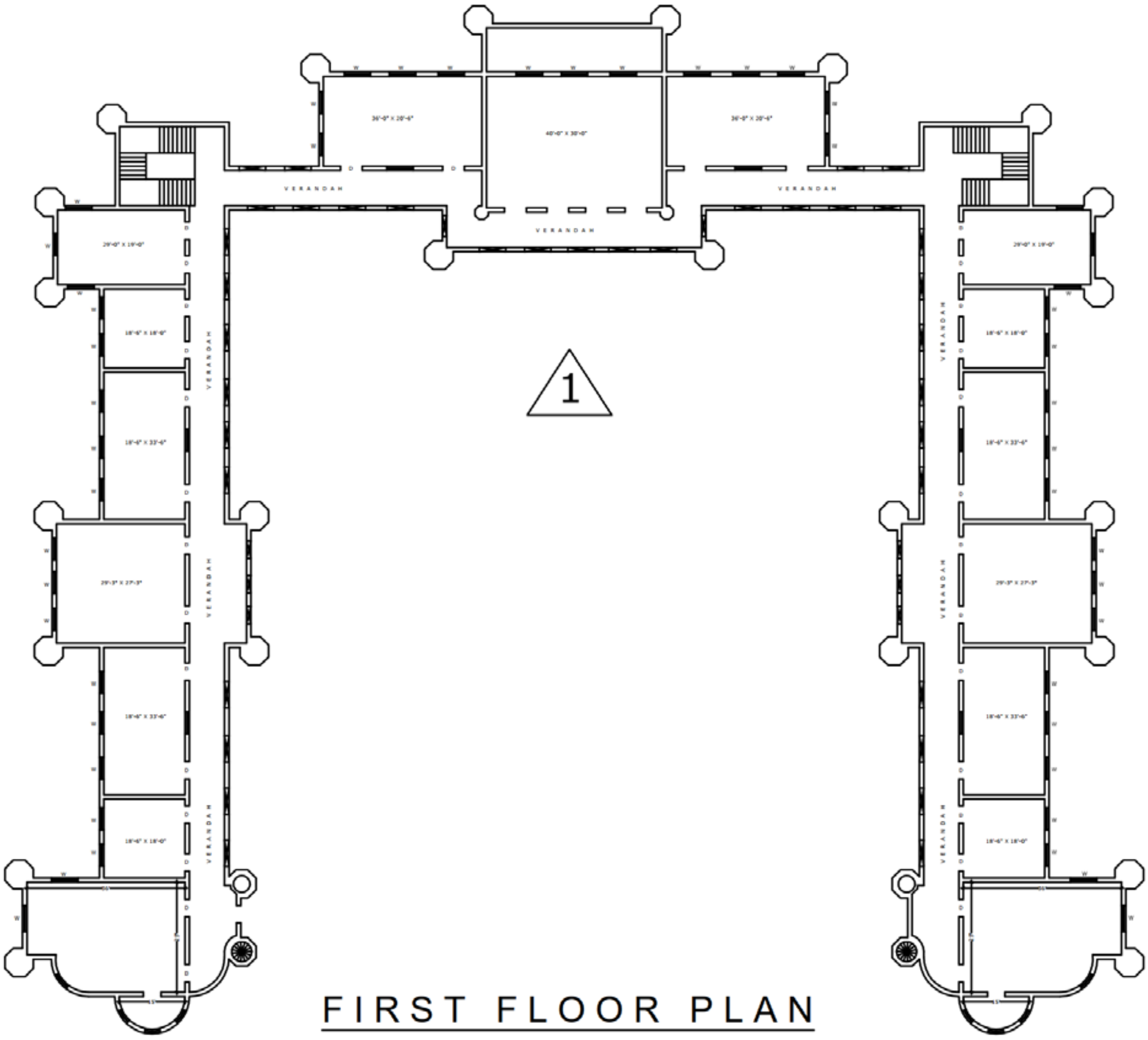

Fig. 4. Typical First Floor Plan

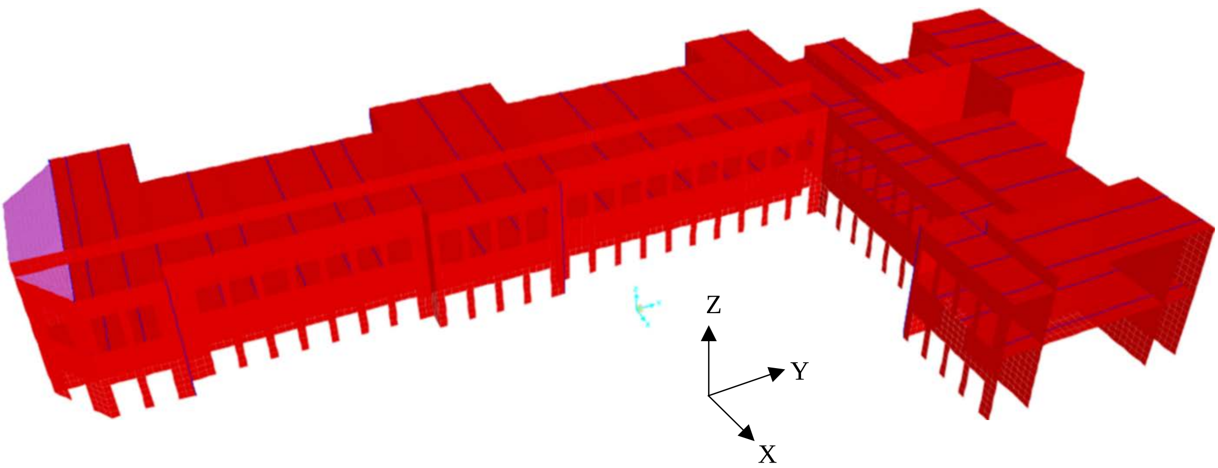

Fig. 5. 3D view of the half structure

4. Analysis and Discussion

In order to examine the exact nonlinear behavior of structures, a nonlinear time history analysis has to be carried out. In this method, the ground motion record is applied to the structures in the form of time history. Chamoli earthquake in the form of ground acceleration has a magnitude of 6.5 on the Richter scale and was recorded at an epicentral distance of 8.72 km. Figure 6 shows the recorded time history data of Chamoli Earthquake. This time history follows the provisions given in FEMA P695 [24], therefore it is used as input ground motion for the analysis.

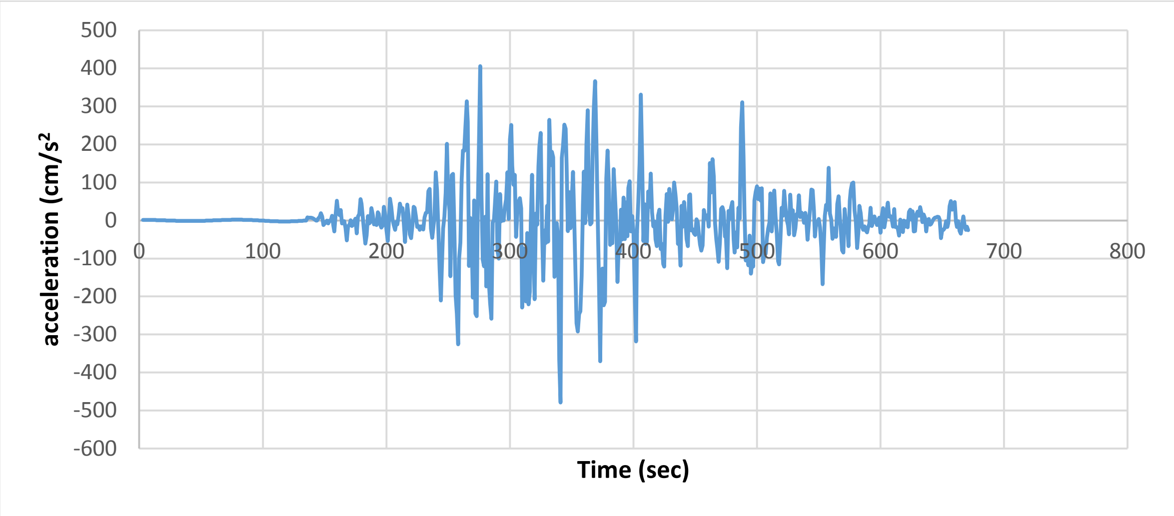

Fig. 6. Time history of Chamoli Earthquake

According to FEMA 273 [25], in order to determine the mechanical properties of existing masonry, test prisms shall be extracted from an existing wall and tested in compression, tension, etc. Since the structure in the present study is a heritage institutional building; it was not allowed to extract the prism from there. In absence of the actual data for the existing building, material properties have been taken after studying the literature. The values taken for old unreinforced brick masonry with lime mortar do not show much variation worldwide. According to F. Paris [26], values of compressive strength and modulus of Elasticity for Old brick masonry with lime mortar can be taken as 2.40 - 4.00 MPa and 1200 - 1800 MPa respectively.

The material properties as shown in Table 1 have been taken from recent literature [27] on seismic analysis of a hundred years old unreinforced masonry buildings in Nepal. The building is having much similarities, in age, construction type and material, etc., with the presently studied building. Also, Nepal is located very near so a similarity can be observed in the material, workmanship, techniques, climate, and other structural parameters. So using the same material properties for the present study is justified. With these data, the heritage building is analyzed using SAP2000 software [28].

Table 1. Mechanical properties of the materials [27]

Materials	Young's Modulus, *E* (N/mm2)	Poisson Ratio, μ	Mass Density (kN/m3)	Compressive Strength (MPa)	Tensile Strength, (MPa)
Brick Masonry	1708	0.15	21	4	0.4

Materials are said to be orthotropic when their properties are different in three mutually perpendicular directions. For the present orthotropic analysis, the values of elastic and shear moduli in three perpendicular directions are taken such that the equivalent of these are nearly equal to isotropic moduli. The values of moduli are given below in Table 2. The values of other required parameters are taken the same as given in Table 1.

Table 2. Material Parameters

Properties of material	Case 1	Case 2	Case 3
E_x (MPa)	1200	800	1000
E_y (MPa)	1000	1200	800
E_z (MPa)	800	1000	1200
G_x (MPa)	500	300	400
G_y (MPa)	400	500	300
G_z (MPa)	300	400	500

Using the above material properties, various modes shapes, and stresses in the structure are obtained from the finite element model.

Natural frequencies and mode shapes of the building have been obtained through modal analysis. The first 3 natural frequencies and corresponding time periods of each case of analysis are given in Table 3. The mode shapes of the case study building are similar for each case. The first three mode shapes are shown in Fig. 7. The natural frequencies decrease and time period increase (Table 3). In each case, the natural frequencies are closely spaced.

Table 3. Natural Frequencies with corresponding time periods

Mode	Isotropic material Case		Orthotropic material case					
			Case 1		Case 2		Case 3	
	Frequency (Cycles/ sec)	Time Period (sec)	Frequency (Cycles/ sec)	Time Period (sec)	Frequency (Cycles/ sec)	Time Period (sec)	Frequency (Cycles/ sec)	Time Period (sec)
1	8.35348	0.11971	6.62155	0.15102	6.17824	0.16186	5.92898	0.16866
2	8.75714	0.11419	6.95845	0.14371	6.21843	0.16081	6.23321	0.16043
3	8.87935	0.11262	7.12476	0.14036	6.43689	0.15535	6.37783	0.15679

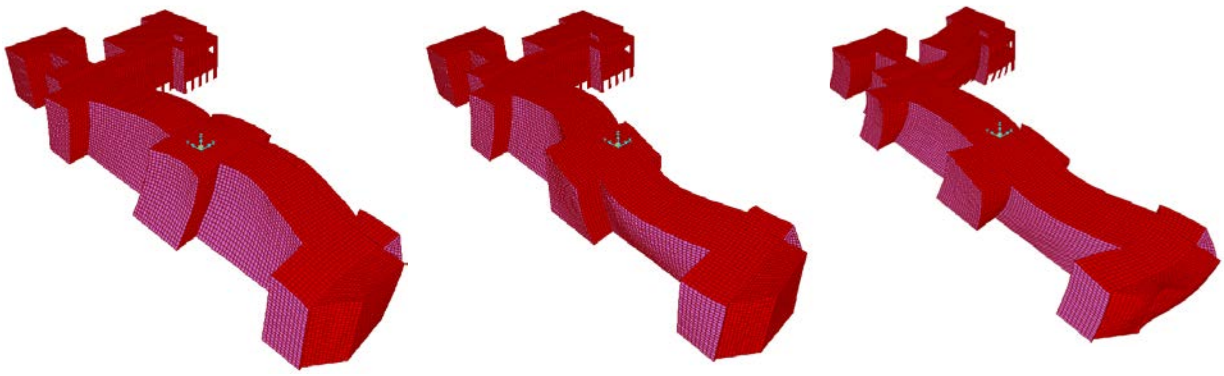

(a) Mode shape I (b) Mode Shape II (c) Mode Shape III

Fig. 7. First Three Natural Mode Shape

The time history in the form of ground acceleration is applied in X and Y directions. The direct principal and maximum shear stresses for different parts of the structure are found. The permissible values of the stresses are given in IS-1905 [29]. For the present case, the permissible values of compressive, tensile, and shear stresses can be taken as 1.1 MPa, 0.07 MPa, and 0.25 MPa respectively.

For Isotropic Material Case. As shown in Fig. 8, most part of the structure remains under compression within a permissible limit. The maximum values of compressive and tensile stresses are found to be 0.810 MPa and 0.222 MPa respectively. The tensile stresses are exceeded at slab and beam wall junctions. As shown in Fig. 9, the structure is experiencing shear stress within a permissible limit i.e. within 0.25 MPa. The maximum value of shear stress is found to be 0.130 MPa.

As shown in Fig. 10, here also most part of the structure remains under compression within a permissible limit. The maximum values of compressive and tensile stresses are found to be 0.818 MPa and 0.254 MPa respectively. The tensile stress is exceeded at all the joints and roofs. As shown in Fig. 11, the structure is having shear stress within permissible limits. The maximum value of shear stress is found to be 0.132 MPa.

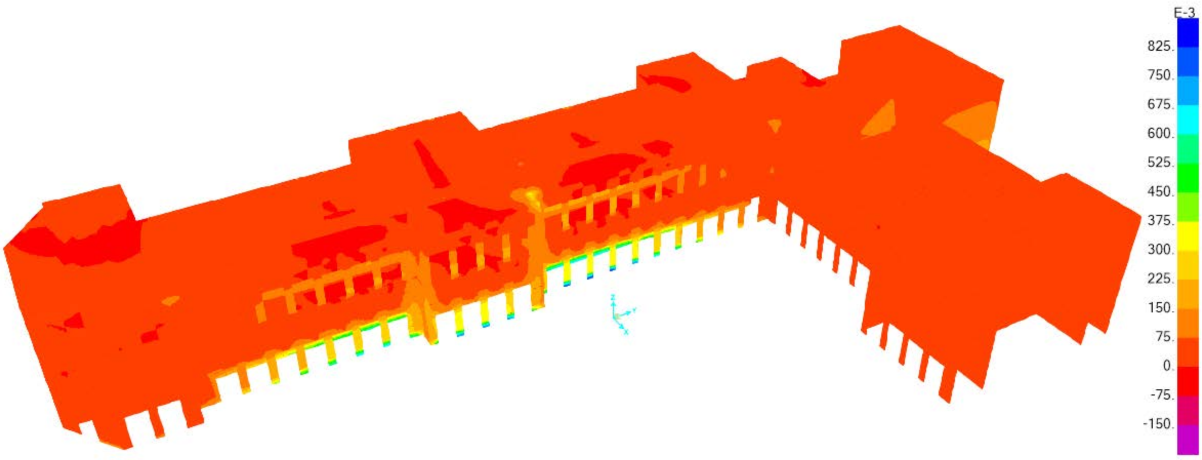

Fig. 8. Direct Principle Stress (MPa) due to Earthquake in X direction in isotropic case

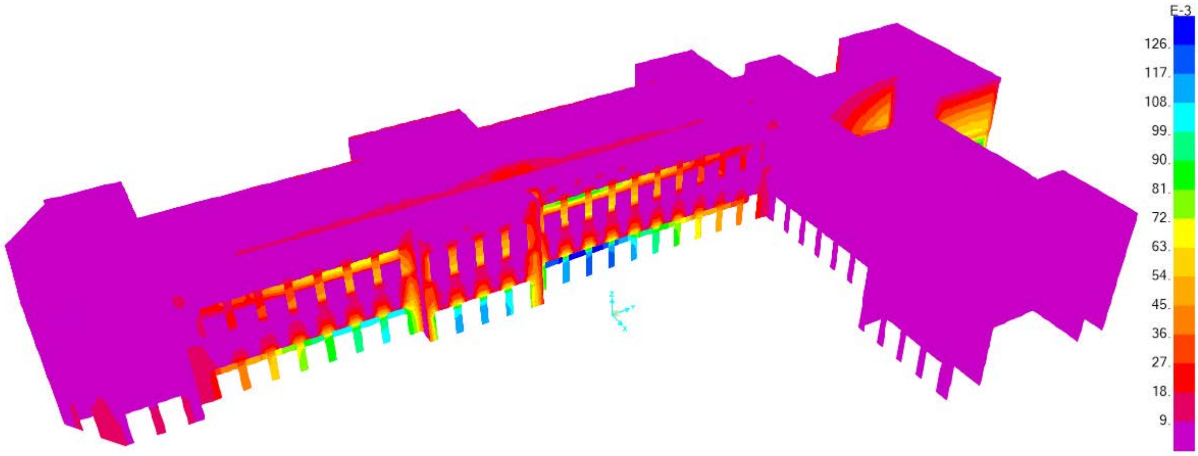

Fig. 9. Maximum Shear Stress (MPa) due to Earthquake in X-direction in isotropic case

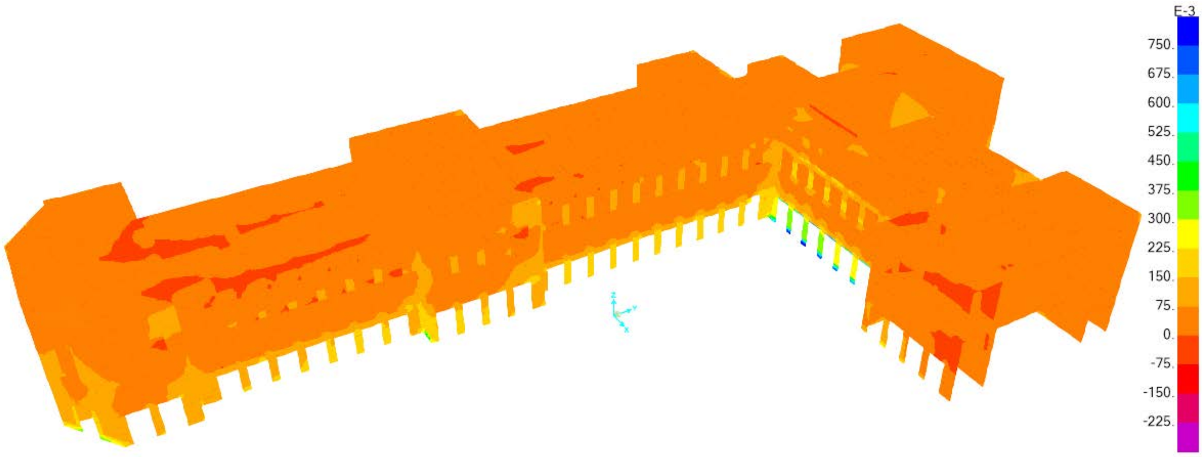

Fig. 10. Direct Principle Stress (MPa) due to Earthquake in Y direction in the isotropic case

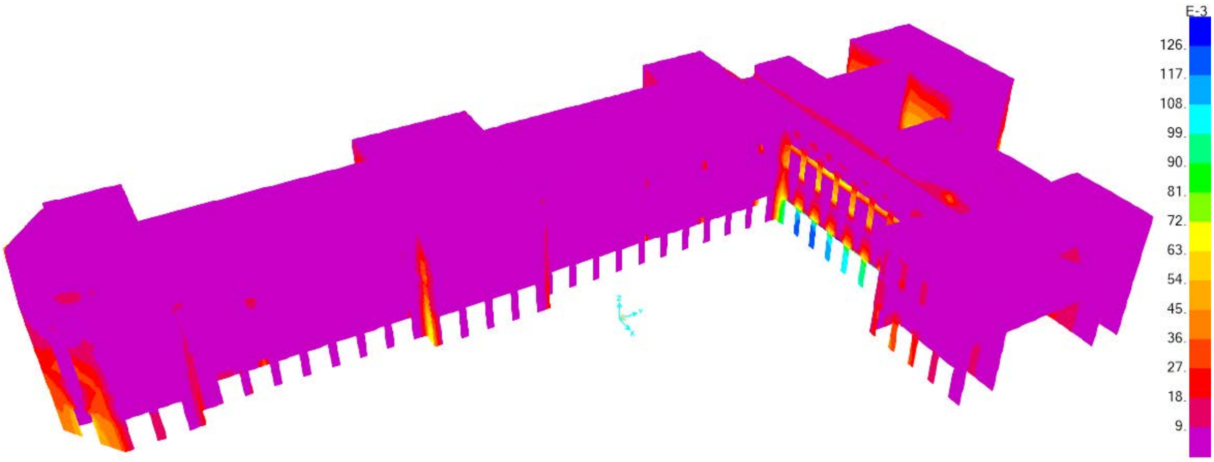

Fig. 11. Maximum Shear Stress (MPa) due to Earthquake in Y-direction in the isotropic case

The shear stress contours in the heritage building were found to be the same in all orthotropic cases when compared to the isotropic material case but the maximum values of the shear stresses were found to be different in each case, therefore, only the maximum value of shear stress has been provided in each orthotropic case. On the other hand, the direct principal stress contours were found to be different from each other with their maximum values, therefore, the figures of direct stress contour results have been provided in each respective case.

For Orthotropic: Case 1. As shown in Fig. 12, most part of the structure remains under compression within a permissible limit. The maximum values of compressive and tensile stresses are found to be 0.618 MPa and 0.206 MPa respectively. The tensile stress is exceeded at roof and beam-wall junctions. The shear stress contours were found to be the same as shown in Fig. 9, however, the maximum value of shear stress is found to be 0.099 MPa, which is within a permissible limit, i.e. 0.25 MPa.

As shown in Fig. 13, here also most part of the structure remains under compression within a permissible limit. The maximum values of compressive and tensile stresses are found to be 0.694 MPa and 0.199 MPa respectively. The tensile stress is exceeded at all the joints and roofs. The shear stress contours were found to be the same as shown in Fig. 11, however, the maximum value of shear stress is found to be 0.111 MPa, which is within a permissible limit.

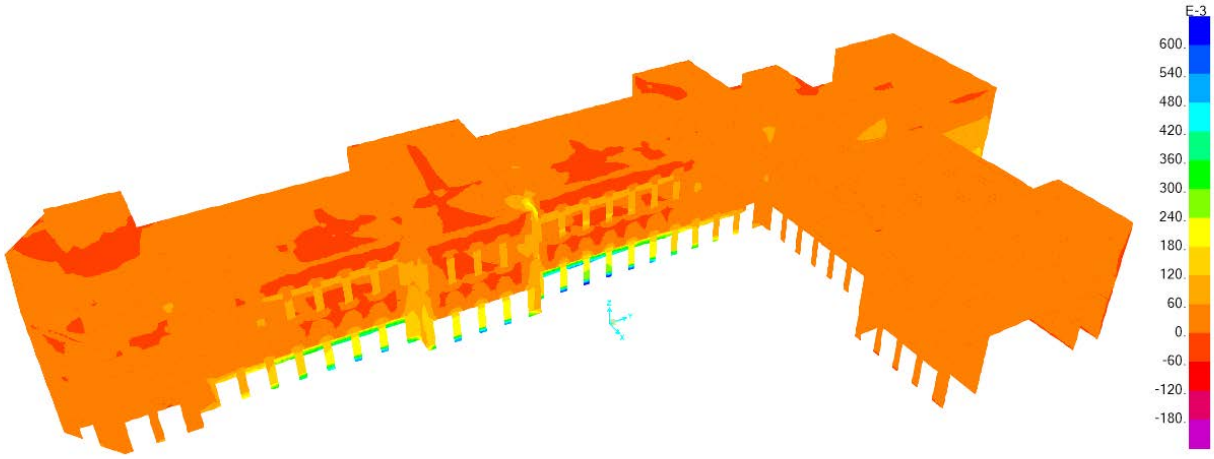

Fig. 12. Direct Principle Stress (MPa) due to Earthquake in X direction in orthotropic case I

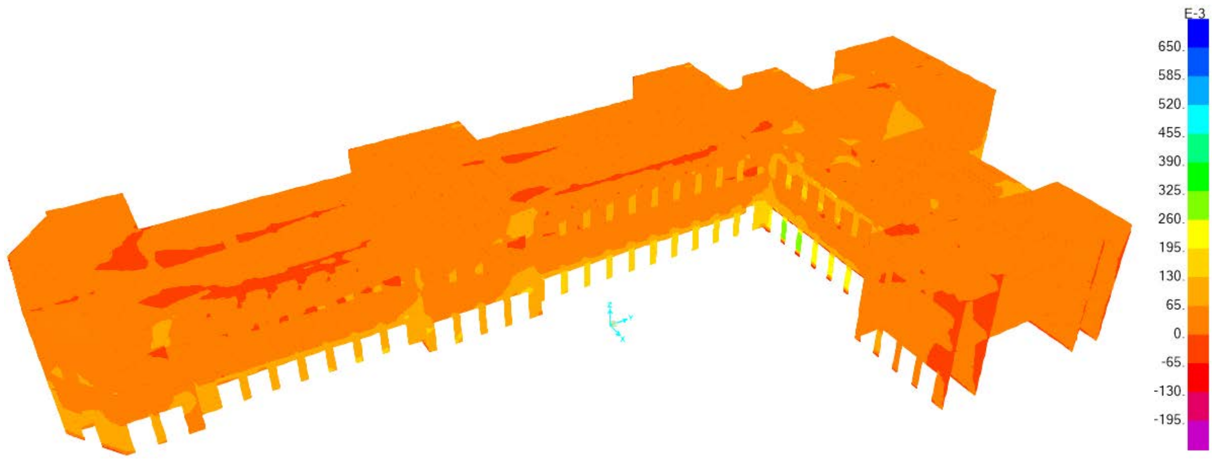

Fig. 13. Direct Principle Stress (MPa) due to Earthquake in Y direction in orthotropic case I

For Orthotropic: Case 2. As shown in Fig. 14, most part of the structure remains under compression within a permissible limit. The maximum values of compressive and tensile stresses are found to be 0.696 MPa and 0.167 MPa respectively. The tensile stress is exceeded at the roof and beam-wall junction. The shear stress contours were found to be the same as shown in Fig. 9, however, the maximum value of shear stress is found to be 0.113 MPa, which is within a permissible limit, i.e. 0.25 MPa.

As shown in Fig. 15, here also most part of the structure remains under compression within a permissible limit. The maximum values of compressive and tensile stresses are found to be 0.687 MPa and 0.196 MPa respectively. The tensile stress is exceeded at all the joints and roofs. The shear stress contours were found to be the same as shown in Fig. 11, however, the maximum value of shear stress is found to be 0.120 MPa, which is within a permissible limit.

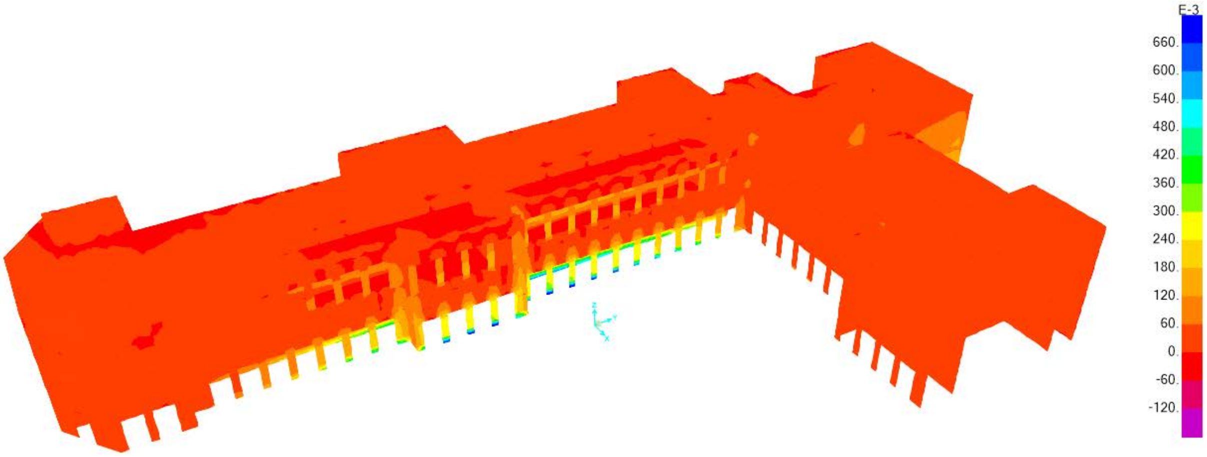

Fig. 14. Direct Principle Stress (MPa) due to Earthquake in X direction in orthotropic case II

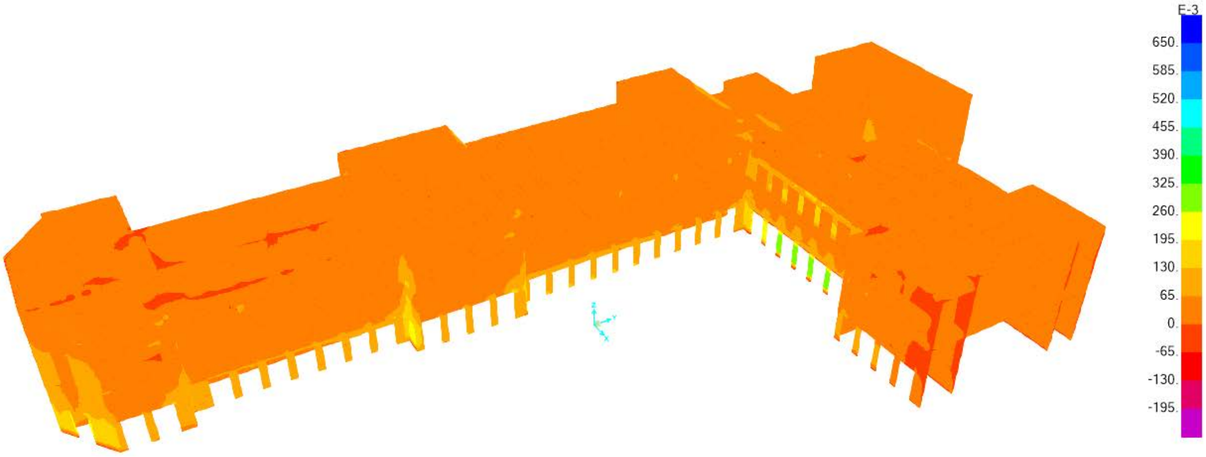

Fig. 15. Direct Principle Stress (MPa) due to Earthquake in Y direction in orthotropic case II

For Orthotropic: Case 3. As shown in Fig. 16, most part of the structure remains under compression within a permissible limit. The maximum values of compressive and tensile stresses are found to be 0.565 MPa and 0.193 MPa respectively. The tensile stress is exceeded at the roof and beam-wall junction. The shear stress contours were found to be the same as shown in Fig. 9, however, the maximum value of shear stress is found to be 0.091 MPa, which is within a permissible limit, i.e. 0.25 MPa.

As shown in Fig. 17, here also most part of the structure remains under compression within a permissible limit. In a few places, the maximum values of compressive and tensile stresses are found to be 0.605 MPa and 0.175 MPa respectively. The tensile stress is exceeded at all the joints and roofs. The shear stress contours were found to be the same as shown in Fig. 9, however, the maximum value of shear stress is found to be 0.097 MPa, which is within a permissible limit.

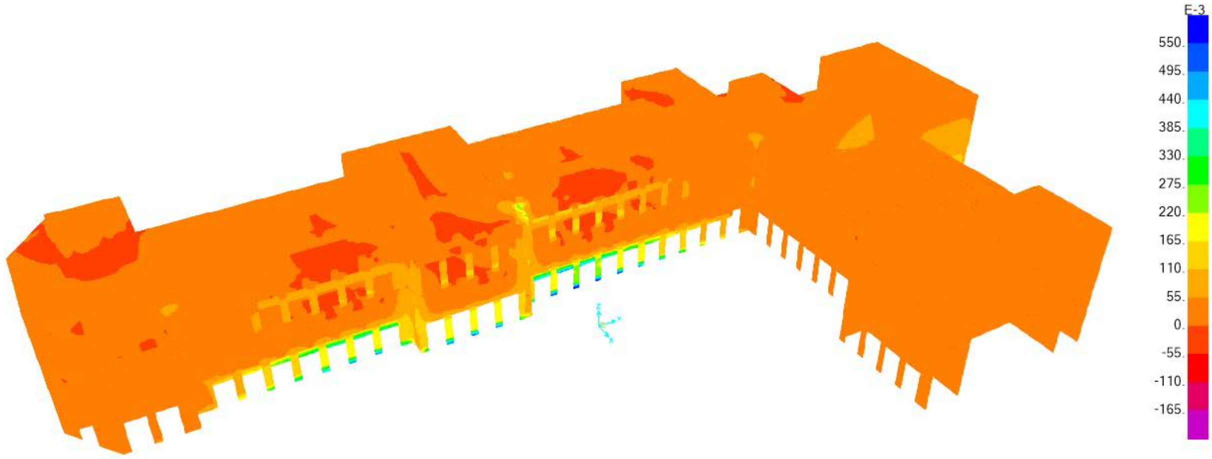

Fig. 16. Direct Principle Stress (MPa) due to Earthquake in X direction in orthotropic case III

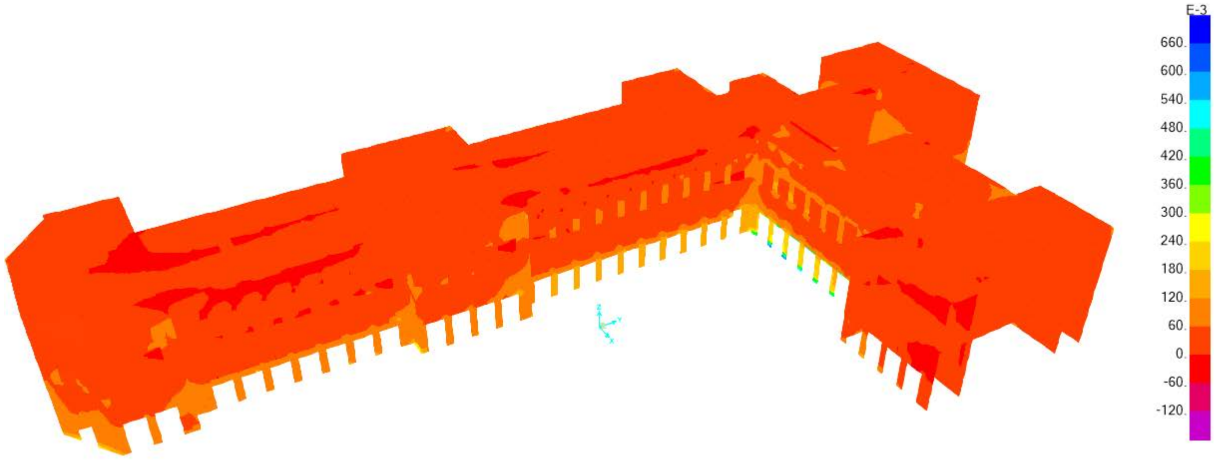

Fig. 17. Direct Principle Stress (MPa) due to Earthquake in Y direction in orthotropic case III

Table 4. Maximum value of Stresses due to Earthquake in X direction

Type of Stress	Isotropic material Case	Orthotropic material cases		
		Case 1	Case 2	Case 3
Compressive (MPa)	0.810	0.618	0.696	0.565
Tensile (MPa)	0.222	0.206	0.167	0.193
Shear (MPa)	0.130	0.099	0.113	0.091

Table 5. Maximum value of Stresses due to Earthquake in Y direction

Type of Stress	Isotropic material Case	Orthotropic material cases		
		Case 1	Case 2	Case 3
Compressive (MPa)	0.818	0.694	0.687	0.605
Tensile (MPa)	0.254	0.199	0.196	0.175
Shear (MPa)	0.132	0.111	0.120	0.097

5. Conclusion

The present study shows that the mode shapes of all cases of analysis are found to be similar (Fig. 6) and their corresponding natural frequencies are closely spaced in each material case, see Table 3. But the values of natural frequencies of the isotropic cases have been found higher than all orthotropic cases. In orthotropic cases, the value of natural frequencies of case 1 is found to be higher than case 2, and case 2 values are found to be higher than case 3.

Due to the earthquake in X-direction, see Table 4, the maximum value of compressive, tensile, and shear stresses of the isotropic cases are found to be higher than the values of all orthotropic cases. The maximum value of compressive stress of orthotropic case 2 value is found to be higher than case 1 and case 1 value is found to be higher than the case 3 whereas the maximum value of tensile stress of orthotropic case 1 value is found to be higher than case 3 and case 3 value is found to be higher than the case 1 whereas the maximum value of shear stress of orthotropic case 2 value is found to be higher than case 1 and case 1 value is found to be higher than the case 2.

Due to the earthquake in Y-direction, see Table 5, the maximum value of compressive, tensile, and shear stresses of the isotropic cases are found to be higher than the values of all orthotropic cases. The maximum value of compressive stress of orthotropic case 1 value is found to be higher than case 2, and case 2 value is found to be higher than case 3. Similarly, the maximum value of tensile stress of orthotropic case 1 is found to be higher than case 2, and case 2 value is found to be higher than case 3 whereas the maximum value of shear stress of orthotropic case 2 value is found to be higher than case 1, and case 1 value is found to be higher than case 3.

In all cases of analysis, the tensile stresses are exceeded the permissible limit whereas the compressive and shear stresses are found to be within the permissible limit. The tensile stresses are exceeded mostly at the corners of walls, roof level, and beam-wall junctions. The maximum value of compressive stress in all cases is found to be at the bottom of walls and piers whereas the maximum value of shear stress is found to be at the corners of walls and piers.

The portions around the openings are found highly vulnerable. There is a requirement for retrofitting to overcome the exceeded stresses.

References

1. Sayin E, Yon B, Calayir Y, Gor M. Construction failures of masonry and adobe buildings during the 2011 Van earthquakes in Turkey. *Structural Engineering and Mechanics*. 2014;51(3): 503-518.

2. Ferreira TM, Vicentea R, Varum H. Seismic vulnerability assessment of masonry facade walls: development, application and validation of a new scoring method. *Structural Engineering and Mechanics*. 2014;50(4): 541-561.

3. Adhikari BR. *Gorkha Earthquake 2015: Cause and Effect*. A CESS NEPAL Publication; 2015.

4. Maio R, Estêvão JM, Ferreira TM, Vicente R. The seismic performance of stone masonry buildings in Faial island and the relevance of implementing effective seismic strengthening policies. *Engineering Structures*. 2017;141: 41-58.

5. Orlando M, Betti M, Spinelli P. Assessment of structural behaviour and seismic retrofitting for an Italian monumental masonry building. *Journal of Building Engineering*. 2020;29: 101115.

6. Altin S, Kuran F, Anil O, Kara ME. Rehabilitation of heavily earthquake damaged masonry building using steel straps. *Structural Engineering and Mechanics*. 2008;30(6): 651-664.

7. Wang Q, Chai Z, Wang L. Seismic capacity of brick masonry walls externally bonded

GFRP under in-plane loading. *Structural Engineering and Mechanics*. 2014;51(3): 413-431.
8. Ortega J, Vasconcelos G, Rodrigues H, Correia M. Assessment of the influence of horizontal diaphragms on the seismic performance of vernacular buildings. *Bulletin of Earthquake Engineering*. 2018;16(9): 3871-904.
9. Ahmad S, Khan RA, Gupta H. Seismic performance of a masonry heritage structure. *Int J Eng Adv Technol*. 2014;3(4): 335-340.
10. Maio R, Ferreira TM, Estêvão JM, Pantò B, Calio I, Vicente R. Seismic performance-based assessment of urban cultural heritage assets through different macro element approaches. *Journal of Building Engineering*. 2020;29: 101083.
11. Couto R, Bento R, Gomes RC. Seismic performance and fragility curves of historical residential buildings in Lisbon downtown affected by settlements. *Bulletin of Earthquake Engineering*. 2020;18(11): 5281-5307.
12. Makoond N, Pelà L, Molins C. A Risk Index for the Structural Diagnosis of Masonry Heritage (RISDiMaH). *Construction and Building Materials*. 2021;284: 122433.
13. Camathias U. *Seismic Performance Evaluation of a Historic Unreinforced Masonry Building Structure. Master Thesis*. Ljubljana, Slovenia: Swiss Federal Institute of Technology, Institute of Structural Engineering, University of Ljubljana; 2013.
14. Sirajuddin M, Sunil J. Narayanan Sambu Potty. Non Linear seismic analysis of masonry structures. *Journal of Design and Built Environment*. 2012;9(1).
15. Capozucca R. Shear behaviour of historic masonry made of clay bricks. *The Open Construction & Building Technology Journal*. 2011;5(1): 89-96.
16. DeJong MJ. *Seismic assessment strategies for masonry structures. PhD Thesis*. USA: Massachusetts Institute of Technology; 2009.
17. Sarhosis V, Asteris PG, Mohebkhah A, Xiao J, Wang T. Three dimensional modelling of ancient colonnade structural systems subjected to harmonic and seismic loading. *Structural Engineering and Mechanics*. 2016;60(4): 633-653.
18. Parajuli HR, Kiyono J, Taniguchi H, Toki K, Furukawa A, Maskey PN. Parametric study and dynamic analysis of a historical masonry building of Kathmandu. *Disaster Mitigation of Cultural Heritage and Historic Cities*. 2010;4(1): 149-156.
19. Sharma A, Golubev VI, Khare RK. Seismic Evaluation of Two-Storied Unreinforced Masonry Building with Rigid Diaphragm Using Nonlinear Static Analysis. In*: Smart Modelling for Engineering Systems.* Singapore: Springer; 2021. p.175-187.
20. Favorskaya A, Golubev V. Study the elastic waves propagation in multistory buildings, taking into account dynamic destruction. In: *Proc. International Conference on Intelligent Decision Technologies.* Singapore: Springer; 2020. p.189-199.
21. Kamran, Ahmad S, Khan RA. Seismic Performance of a heritage school building. *Procedia engineering*. 2017;173: 1763-1770.
22. Lourenço PB. Computations on historic masonry structures. *Progress in Structural Engineering and Materials*. 2002;4(3): 301-319.
23. Kheirollahi M. Equivalent frame model and shell element for modeling of in-plane behavior of Unreinforced Brick Masonry buildings. *Structural Engineering and Mechanics*. 2013;46(2): 213-229.
24. *Quantification of Building Seismic Performance Factors*. Washington DC: Federal Emergency Management Agency; 2009.
25. *Guidelines for the seismic rehabilitation of buildings*. Washington DC: Federal Emergency Management Agency; 1997
26. Parisi F, Augenti N. Experimental data analysis for mechanical modelling of existing brick masonry structures. In: *15 WCEE*. LISBOA; 2012.
27. Khadka SS. Seismic performance of traditional unreinforced masonry building in Nepal. *Kathmandu University Journal of Science and Technology*. 2013;9(1): 15-28.

28. *SAP2000. Reference Manual. Computers and Structures.* Berkeley: University of Ave; 2015.
29. Standard I. *Code of practice for structural use of unreinforced masonry*. New Delhi: Bureau of Indian Standards: 1987.

THE AUTHORS

Kamran
e-mail: kmrn890@gmail.com
ORCID: 0000-0001-6456-3089

Shakeel Ahmad
e-mail: shakeel60in@yahoo.co.in
ORCID: 0000-0002-9516-3296

Rehan A. Khan
e-mail: rehan_iitd@rediffmail.com
ORCID: 0000-0001-6891-9521